

Domain state model for exchange bias

U. Nowak,^{a)} A. Misra, and K. D. Usadel

Theoretische Tieftemperaturphysik, Gerhard-Mercator-Universität Duisburg, 47048 Duisburg, Germany

Monte Carlo simulations of a system consisting of a ferromagnetic layer exchange coupled to a diluted antiferromagnetic layer described by a classical spin model show a strong dependence of the exchange bias on the degree of dilution in agreement with recent experimental observations on Co/CoO bilayers. These simulations reveal that diluting the antiferromagnet leads to the formation of domains in the volume of the antiferromagnet carrying a remanent surplus magnetization which causes and controls exchange bias. To further support this domain state model for exchange bias we study, in the present article, the dependence of the bias field on the thickness of the antiferromagnetic layer. It is shown that the bias field strongly increases with increasing film thickness and eventually goes over a maximum before it levels out for large thicknesses. These findings are in full agreement with experiments.

For a ferromagnet (FM) in contact with an antiferromagnet (AFM) a shift of the hysteresis loop along the magnetic field axis can occur which is called exchange bias (EB). Usually, EB is observed after cooling the system with the FM magnetized in saturation below the Néel temperature T_N of the AFM or after cooling the entire system in an external magnetic field. Although this effect has been well known for many years^{1,2} its microscopic origin is still discussed controversially. For a review see a recent article by Nogués and Schuller.³

In a previous article⁴ we reported on EB observed experimentally in Co/CoO bilayers as a function of volume defects in the antiferromagnet. Of particular importance in this study was the observation that it is possible to strongly influence EB in Co/CoO bilayers by diluting the antiferromagnetic CoO layer, i.e., by inserting nonmagnetic substitutions ($\text{Co}_{1-x}\text{Mg}_x\text{O}$) or defects (Co_{1-y}O) not at the FM/AFM interface, but rather throughout the volume part of the AFM. While the undiluted samples show only a very small EB, dilution increases EB dramatically. Since, for all samples investigated, a 0.4 nm thick CoO layer with minimum defect concentration was placed at the interface the observed EB is not primarily due to disorder or defects at the interface. Rather, the full antiferromagnetic layer must be involved and we have argued that our systems EB has its origin in a domain state in the volume part of the AFM which triggers the spin arrangement and thus the FM/AFM exchange interaction at the interface. Indeed, in diluted antiferromagnets when cooled in external fields metastable domains occur carrying a surplus magnetization and having very slow dynamics.^{5,6} These domains are frozen to a large extent during hysteresis cycles and their frozen magnetization is the origin of EB. This domain state model for EB was supported by large scale Monte Carlo simulations performed at finite temperatures.⁴

To gain additional evidence for the domain state model in the present article we will concentrate on the dependence

of EB on the thickness of the AFM. The system consists of a FM monolayer exchange coupled to a diluted AFM layer with t monolayers. The FM is described by a classical Heisenberg model with vector spins \underline{S}_i and exchange constant J_{FM} . The dipolar interaction is approximated by an additional anisotropy term (anisotropy constant $d_x = -0.1J_{\text{FM}}$) which mimics the shape anisotropy leading to a magnetization which is preferentially in the y - z plane. Also, we introduce an easy axis in the FM (z axis, anisotropy constant $d_z = 0.1J_{\text{FM}}$) in order to obtain well defined hysteresis loops. d_z sets the Stoner–Wohlfarth limit of the coercive field, i.e., the zero temperature limit for magnetization reversal by coherent rotation ($B_{\text{SW}} = 2d_z$, in our units, for a field parallel to the easy axis). In view of the rather strong anisotropy in CoO we assume an Ising Hamiltonian for the AFM. Thus, the Hamiltonian of our system is given by

$$\begin{aligned} \mathcal{H} = & -J_{\text{FM}} \sum_{\langle i,j \rangle} \underline{S}_i \cdot \underline{S}_j - \sum_i (d_z S_{iz}^2 + d_x S_{ix}^2 + \underline{S}_i \cdot \underline{B}) \\ & - J_{\text{AFM}} \sum_{\langle i,j \rangle} \epsilon_i \epsilon_j \sigma_i \sigma_j - \sum_i B \epsilon_i \sigma_i - J_{\text{INT}} \sum_{\langle i,j \rangle} \epsilon_i \sigma_i S_{jz} \end{aligned} \quad (1)$$

with the antiferromagnetic nearest-neighbor exchange constant $J_{\text{AFM}} < 0$ and the effective in-plane magnetic field $\underline{B} = B_x \hat{x} + B_y \hat{y}$. The values of the magnetic moments are incorporated in B and d , respectively, so that the quantities \underline{S}_i denote unit vectors and $\sigma_i = \pm 1$ Ising spin variables. A fraction p of the sites of the lattice is left without a spin (quenched disorder: $\epsilon_i = 0, 1$). For the exchange constant of the AFM which mainly determines its Néel temperature (also depending on the dilution, of course) we set $J_{\text{AFM}} = -J_{\text{FM}}/2$. There seems to be some evidence that the exchange coupling between Co and CoO is ferromagnetic⁷ but its strength is not known experimentally. Therefore, we assume in our simulations a ferromagnetic coupling with ($J_{\text{INT}} = -J_{\text{AFM}}$).

We use Monte Carlo methods with a heat-bath algorithm and single-spin flip methods for the simulation of the model explained above. The trial step of the spin update is a small

^{a)}Electronic mail: uli@thp.uni-duisburg.de

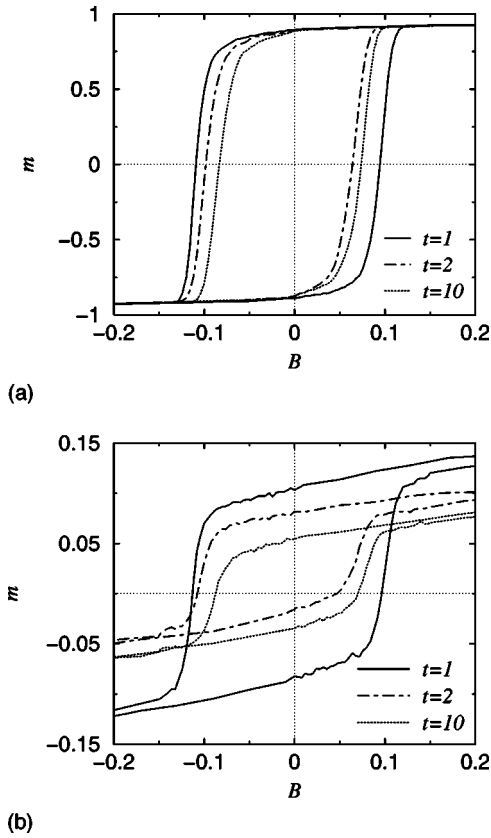
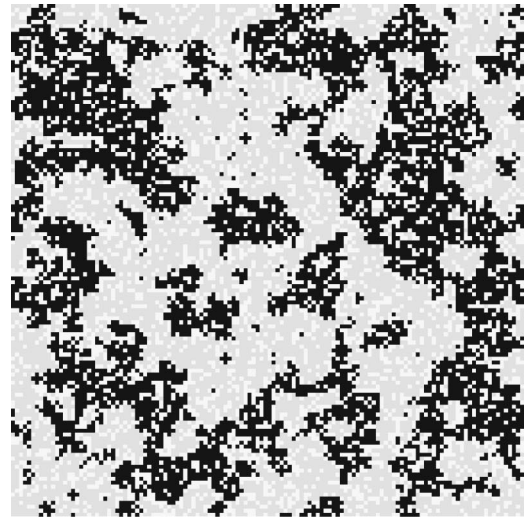


FIG. 1. Simulated hysteresis loops of the model explained in the text for $p=0.4$ and $k_B T=0.1J_{\text{FM}}$. The field during cooling was $0.25J_{\text{FM}}$. Shown is the net magnetization in units of the saturation magnetization of the FM (upper figure) and of the interface monolayer of the AFM (lower figure) for different thicknesses t of the AFM.

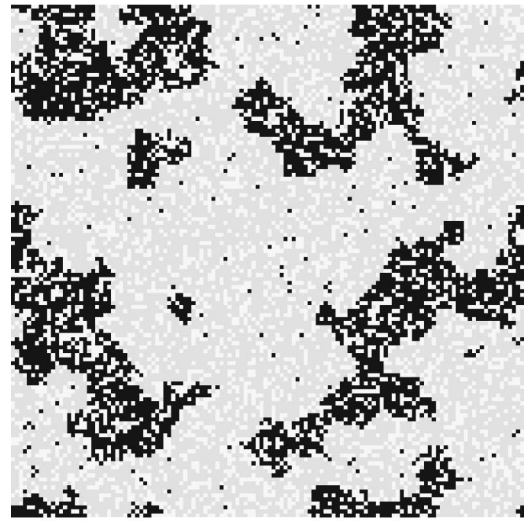
variation around the initial spin for the Heisenberg spins and—as usual—a spin flip for the Ising spins.⁸ We perform typically 40000 Monte Carlo steps per spin for a complete hysteresis loop. To observe the domain structure of the AFM we have to guarantee that typical length scales of the domain structure fit into our system. For the parameter values used in this simulation this is achieved for systems of lateral extension 128×128 .

In the simulations the system is cooled from above to below the ordering temperature of the AFM in an applied external cooling field $\underline{B} = B_c \hat{z}$ with $B_c = 0.25J_{\text{FM}}$. The FM is then long-range ordered and its magnetization is practically homogeneous resulting in a nearly constant exchange field for the AFM monolayer at the interface. When the desired final temperature is reached a magnetic field $\underline{B} = B_z \hat{z} + B_y \hat{y}$ is applied which also has a small constant perpendicular field component $B_y = 0.05J_{\text{FM}}$ in order to define a certain path for the rotation of the magnetization during field reversal and to avoid the system to be trapped in a metastable state. The z component of the field \underline{B} is then reduced in steps of $\Delta B = 0.004J_{\text{FM}}$ from $B = 0.2J_{\text{FM}}$ down to $-B$ and afterwards raised again up to the initial value.

Typical hysteresis loops are depicted in Fig. 1. Shown are results for the magnetization of the FM (upper figure) as well as that of the AFM interface monolayer (lower figure) for different thicknesses t of the AFM. The hysteresis loops



(a)



(b)

FIG. 2. Frozen domain states of the AFM. Shown are staggered spin configurations (gray and black) of the AFM interface layer after the initial cooling procedure for dilution $p=0.3$. AFM thickness $t=1$ (upper figure) and $t=10$ (lower figure). Vacancies are left white.

of the FM clearly show EB depending on the thickness of the AFM. The magnetization curves of the interface layer of the AFM are shifted upwards due to the fact that after field cooling the AFM is in a domain state with a surplus magnetization. During cooling this layer was exposed to the external field in addition to the exchange field of the FM both having the same direction. This shifted interface magnetization of the AFM acts as an additional effective field on the FM, resulting in EB. The hysteresis curve of the AFM interface layer follows that of the FM layer with a much lower saturation magnetization, however. With increasing thickness of the AFM layer the area of the hysteresis loop of the interface layer which is proportional to the energy losses in the AFM decreases indicating that the spin structure in the AFM is stabilized.

The domain structure in the AFM interface layer is shown in Fig. 2 for an AFM consisting of 1 ML (upper figure) and for 10 ML (lower figure), respectively. The frac-

tal structure of these domains is obvious. It has been observed previously in bulk systems and was analyzed in detail.^{9,10} The domain structures shown in Fig. 2 are, to a large extent, frozen. But during field cycles small spin arrangements in the domain boundaries can take place even at low temperatures resulting in the hysteresis loops shown in Fig. 1.

The structure of the domains depends on the thickness of the AFM. For an AFM monolayer the effective field acting on all AFM spins is the superposition of the strong exchange field and the external field. But it is well known that the size of the domains depends on the strength of the effective magnetic field. Large fields imply small domains and vice versa.⁹⁻¹³ The small domains seen in the upper part of Fig. 2 are thus due to the strong fields acting on the AFM monolayer. On the other hand if the AFM consists of ten layers nine of them are only exposed to the weak external field with the tendency to form larger domain sizes. The coupling of these layers to the AFM interface layer then results in a coarsening of the domains at the interface as seen in the lower part of Fig. 2. Note that the distribution of vacancies in the interface layer is exactly the same in both parts of Fig. 2. A further obvious consequence of this explanation is that the domain size becomes layer dependent and increases with increasing distance from the AFM interface. But after a certain distance from the interface the domain structure should become independent of the interface layer which means that the bias field should also become independent of the thickness of the AFM for large t . This behavior indeed is observed in our simulations. In Fig. 3 we show the dependence of the bias field on t for different dilutions of the AFM. The bias field is determined as $B_{EB} = (B^+ + B^-)/2$ where B^+ and B^- are those fields of the hysteresis loop branches for increasing and decreasing field where the easy axis component of the magnetization of the FM becomes zero. The absolute value of the bias field increases rapidly with film thickness t , goes eventually over a maximum and then levels out. This is in agreement with experiments.⁷ Note that for the system with the smallest dilution the absolute value of the bias field decreases for $t > 1$ much stronger with increasing thickness than for the more diluted films. The reason is that the less diluted systems have a stronger tendency to order antiferro-

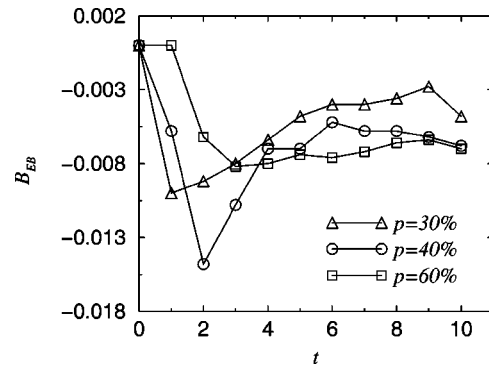


FIG. 3. Exchange bias field vs thickness t of the AFM layer for different values of the dilution.

magnetically thus reducing the net magnetization at the AFM interface. Again, agreement with experiments is obtained.

In conclusion, we have found, by Monte Carlo simulations, further support for our domain state model for exchange bias. So far all our numerical results have been obtained for systems where the AFM has a very strong anisotropy, i.e., behaves Ising-like. It is of great interest to relax this condition, i.e., to consider vector spin models for the AFM. Work in this respect is in progress.

This work has been supported by the Deutsche Forschungsgemeinschaft through SFB 491.

¹W. H. Meiklejohn and C. P. Bean, Phys. Rev. **102**, 1413 (1956).

²W. H. Meiklejohn and C. P. Bean, Phys. Rev. **105**, 904 (1957).

³J. Nogués and I. K. Schuller, J. Magn. Magn. Mater. **192**, 203 (1999).

⁴P. Miltényi, M. Gierlings, J. Keller, B. Beschoten, G. Güntherodt, U. Nowak, and K. D. Usadel, Phys. Rev. Lett. **84**, 4424 (2000).

⁵W. Kleemann, Int. J. Mod. Phys. B **7**, 2469 (1993).

⁶D. P. Belanger, in *Spin Glasses and Random Fields*, edited by A. P. Young (World Scientific, Singapore, 1998).

⁷B. Beschoten, P. Miltényi, J. Keller, and G. Güntherodt (these proceedings).

⁸U. Nowak, in *Annual Reviews of Computational Physics IX*, edited by D. Stauffer (World Scientific, Singapore, 2000), p. 105.

⁹U. Nowak and K. D. Usadel, Phys. Rev. B **46**, 8329 (1992).

¹⁰J. Esser, U. Nowak, and K. D. Usadel, Phys. Rev. B **55**, 5866 (1997).

¹¹Y. Imry and S. Ma, Phys. Rev. Lett. **35**, 1399 (1975).

¹²R. J. Birgeneau, R. A. Cowley, G. Shirane, and H. Yoshizawa, J. Stat. Phys. **34**, 817 (1984).

¹³D. P. Belanger, M. Rezende, A. R. King, and V. Jaccarino, J. Appl. Phys. **57**, 3294 (1985).